Rotary friction welding of molybdenum components

M. Stütz*, F. Pixner*, J. Wagner**, N. Reheis**, E. Raiser***, H. Kestler**, N. Enzinger*

* IMAT, Graz University of Technology, Austria

** Plansee SE, 6600 Reutte, Austria

*** Klaus Raiser GmbH & Co. KG, Germany

Abstract

Joining of TZM components by inertia rotary friction welding is an established industrial process, but only for welding cross-sections up to 1,500 mm^2. Up-scaling to medium-size components up to 5,000 mm^2 in a direct drive variant of the process requires further development and more basic understanding of the welding procedure including weld preforms, the clamping system, and machine parameters.

Based on the existing process for TZM tubes, the welding parameters were transferred to tubular components of pure molybdenum (Ø 130 x 10 mm, 4,400 mm^2). Successful welds were produced showing a fine-grained, defect-free microstructure. However, molybdenum proved to be more challenging than TZM. Particularly high upset rates and motor overload occurred during the friction phase. Therefore, a more mechanism based weld study was carried out with small-size samples under laboratory conditions. The results showed extensive plasticization of the entire weld zone due to higher thermal diffusivity and lower strength of molybdenum compared to TZM. This high upset rate reduces the process window for a reproducible welding procedure significantly. Moreover, a concentrated energy input during the transition from friction to forge phase is required to countervail the high thermal diffusivity of molybdenum. Based on these observations, the feasibility of friction welding of medium-size molybdenum tubes will be discussed.

Keywords

Refractory Metals, Molybdenum, TZM, Welding, Rotary Friction Welding

Introduction

Molybdenum and TZM

Molybdenum (Mo) is a refractory metal of group VI in the periodic table. Its crystal lattice is body-centered cubic and monomorphic. Mo is brittle at room temperature and highly susceptible to traces of impurities, most of all oxygen [1]. Small oxide precipitates are formed and if segregated on the grain

boundaries they lower the ductility. Therefore, minimizing impurities is the goal in the production of Mo and Mo-based alloys [1, 2]. The dispersion strengthened alloy TZM is the most commonly used Mo-alloy. Small additions of titanium, zirconium, and carbon lead to the formation of carbides and act as getter elements for oxygen. As a consequence, recrystallization temperature and high temperature strength are increased compared to technical pure Mo [1]. In the temperature regime between 900 and 1,500 °C the ultimate tensile strength (UTS) of TZM is up to five times higher compared to Mo, and the service temperature for TZM is specified up to 1,400 °C [3].

Welding of molybdenum and TZM includes some general problems. A further embrittlement of the material is observed if joined by fusion welding, for instance TIG welding. The melting and re-solidification causes grain coarsening and re-distribution of impurities and precipitates on the grain boundaries occurs [4, 5]. The technique of friction welding avoids the typical defects of fusion welding and the resulting embrittlement of Mo. Grain size is reduced by high deformation and deformation rates during the process, thus supporting better toughness compared to fusion welding [6, 7].

Friction welding

Friction welding is a solid state joining process, where the required heat is generated by friction caused by a relative movement between the joining partners. When the shear strength is reached, the partners start to plasticize and the characteristic flash starts to form. The physical background of the heat generation is not fully understood, which is the reason why several different models exist. The total heat generation is a combination of friction heating and heating due to plastic deformation. The ratio between these two effects as well as the maximum temperature at the welding interface, however, are still subject to discussion [8–10].

Friction welding variants

In general, two driving concepts exist: inertia friction welding (IFW) and direct drive friction welding (DDFW):

1. In inertia friction welding, the rotary part and an attached flywheel are accelerated to a certain speed, then the drive is decoupled and the welding partners are brought in contact. The motion decelerates during the whole welding process continuously. Towards the rotary halt, the axial force is increased in case of a two-step process.
2. In a direct drive process, a motor drives the rotary welding part during the whole process and at the sudden braking of the rotation, the axial pressure is increased whereby the flash is fully formed and the process is completed shortly after the spindle halt.

Both driving concepts are in industrial-scale application with their inherent advantages and drawbacks [8, 9, 11]. The transferability between IFW and DDFW with respect to welding parameters is discussed in the following section.

Welding parameters for IFW and DDFW and their comparability

The welding parameters in inertia friction welding are the available welding energy $E(t)$, which is stored in the flywheel, and friction pressure $p(t)$. The total process time t_t and initial speed n_0 directly depend

on the before mentioned energy and pressure. Figure 1 represents a typical inertia weld cycle for TZM. Here, the process is divided into two stages with two pressure levels: 39 MPa and 96 MPa. In inertia welding, the heat generated in the friction surface is solely withdrawn from the flywheel, hence the consideration

$$E(t) = \frac{1}{2} \cdot J \cdot \omega^2 \tag{1}$$

$$P(t) = \frac{dE}{dt} = J \cdot \omega \cdot \frac{d\omega}{dt} \tag{2}$$

leads to a simple calculation of the current weld power $P(t)$ as the derivate of angular velocity $\omega(t)$. Figure 1b depicts the calculated weld power and the course of the upset. It is observed that the generated welding power reaches a 200 kW peak early in the process, but the larger upset occurs at lower power levels of 150 kW.

Scaling the size within IFW processes of a certain material can be done using the specific weld energy [12]:

$$\frac{E}{A} = const. \tag{3}$$

In direct drive welding, friction time and speed are independent from friction pressure. Therefore, more welding parameters have to be determined, which may render finding a suitable set of parameters more challenging. In general, welding times are longer and friction pressures are lower owing to the limited torque and motor power [8].

The specific weld energy is the relevant parameter in IFW processes. This parameter can be calculated for DDFW process from the product of motor load and speed over time. However, due to the longer process times of DDFW, the heat dissipation becomes more significant compared to IFW. Defining the relevant time period to calculate the specific energy is essential to allow a rough comparison. As a consequence, a more detailed analysis of the power progression is necessary.

(a)   (b)
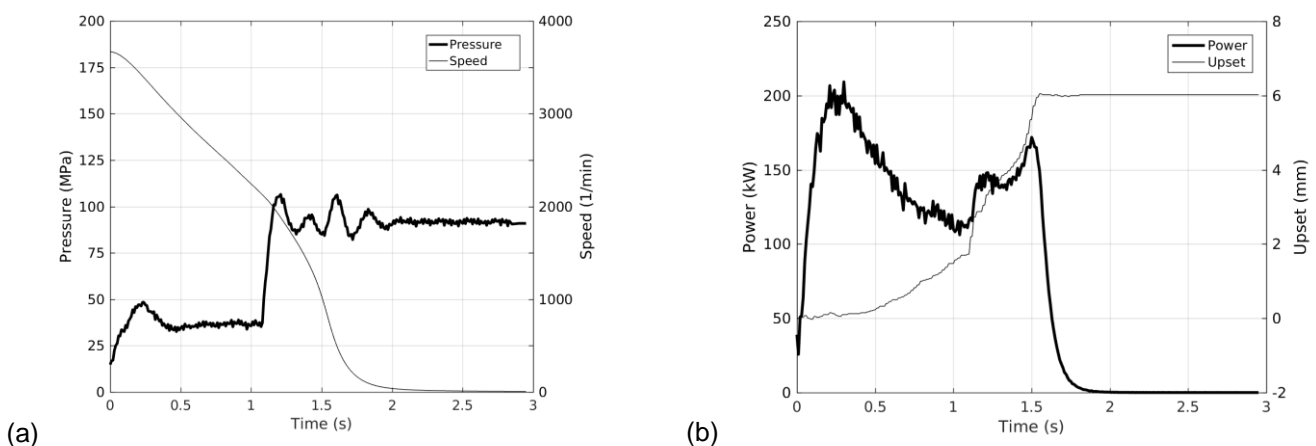
Figure 1:   Typical inertia friction welding process for TZM tubes: (a) Welding parameters pressure and speed and (b) calculated power and upset as response.

Experiments

Material

The investigated materials were commercially pure Mo (> 99.97 wt.%) and TZM (0.5 % Ti, 0.08 % Zr, 0.01–0.04 % C, all wt.%). The production route of the material was sintered, hot forged, stress-relieve annealed, and machined to their final dimensions.

Medium-size tube format

To examine welding of pure Mo tubes with 4,400 mm^2 cross sections (Ø 130 x 10 mm), a heavy-duty direct drive rotary friction welding machine with 150 kW drive power and 1,250 kN maximum forge force was used. Axial force, speed, upset, and motor load parameters were recorded. Investigated parameters were friction pressure, welding speed, and friction time. The Mo tubes were pre-heated in a furnace to 400 °C.

In a first step, process parameters from IFW were used to define the DDFW process for medium-size Mo tubes. As an approximation, the specific weld energy of 156 J/mm^2 of the given IFW process was up-scaled from 1,500 mm^2 to 4,400 mm^2. This resulted in an estimated total weld energy of 686 kJ, which may be achieved in 4.6 s by the present 150 kW drive. To overcome initial torque peaks, a ramp from (minimum controllable) 10 to 20 MPa friction pressure was programmed. In preliminary tests it was observed that the motor cannot keep the nominal welding speed. For this reason a threshold of 250 min^{-1} was defined which initialized the forge phase if the spindle speed fell below this value.

Small-size formats

As a result of the occurring problems in the medium-size experiments, neither a comprehensive parameter recording nor an analysis of the parameter influences were possible. To enable a focus on material behavior during the process, a friction stir welding machine (MTS I-STIR BR4) with comprehensive parameter control and recording was adapted for rotary friction welding (RFW). The machine capabilities were a maximum axial force of 35.6 kN, spindle speed 3,200 min^{-1}, 180 Nm torque, and axial travel of 15 mm. Small-size friction welds with Ø 12 mm rods of Mo and Ø 9 mm rods of TZM material were accomplished.

To exceed the ductile-brittle transition temperature, an in-situ pre-heating phase was developed [13]. Friction at low pressures (< 10 MPa) resulted in a constant temperature distribution (350 °C in 8 mm distance from the weld interface) in the samples without significant plastic deformation. The actual welding process was started by increasing the pressure to friction pressure. Figure 2 depicts the programmed input parameters pressure and speed for Mo and TZM. Varied welding parameters were friction pressure, welding speed, and forge condition to determine optimal welding conditions. The forge condition is determined by three parameters:
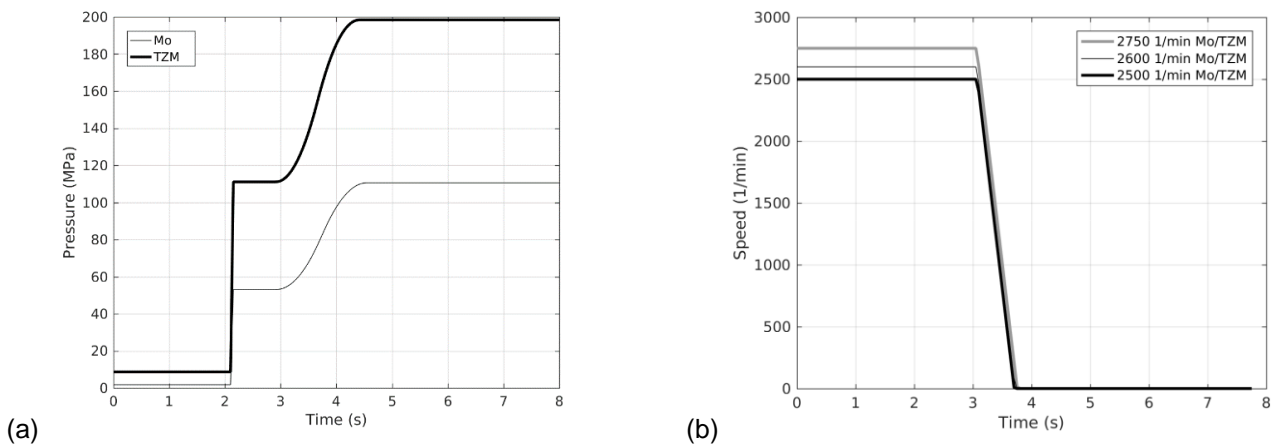
(a) (b)

Figure 2: (a) Input pressure course for Mo and TZM samples. TZM requires a higher pressure level (111 / 200 MPa) than Mo (53 / 110 MPa), due to the elevated high temperature strength. (b) Friction speed was varied between 2,500 and 2,750 min^{-1} to adjust weld energies.

1. Forge point: The initiation of the forge phase in relation to the current spindle speed. In the small-size experiments the forge force was applied upon deceleration start. This is common practice in friction welding [11] and referred to as "forging into the turning spindle."
2. Forge force gradient: The rate of force increase from friction force to forge force with set values between 4 and 50 kN/s.
3. Spindle deceleration: The deceleration rate from welding speed to spindle stop varying from 2,500 to 4,000 min^{-1}s^{-1}.

Characterization

The welded samples were characterized by visual inspection to evaluate the flash shape, the geometric symmetry of the weld and the visual appearance. Metallographic investigations were carried out on welded samples to check the integrity and the microstructure of the welds.

Results

Molybdenum medium-size format

Different trial welds were performed, the welding parameters of one representative weld are shown in Figure 3. This trial has already been published and the friction welding behavior was compared to steel samples [14]. Regardless of the welding parameters, the experiments showed a preliminary spindle stall due to insufficient motor power.

Comparing Figure 3b to Figure 3c reveals that the nominal weld speed of n = 900 min^{-1} decreases immediately when upsetting starts. The upset rate increased up to 7 mm/s during the friction phase, which is notable high compared to other materials (e.g. a maximum of 3.5 mm/s has been reported for Ø 20 mm steel rods [15]). As a result, the plasticizing material caused a large power demand which exceeded the accessible drive power. The spindle halt can be also observed by the small plateau in the upset course at t = 4 s (Figure 3c). In this event the friction pressure was still applied at no spindle motion. The increase to forge pressure at t = 4.5 s enlarged the upset.
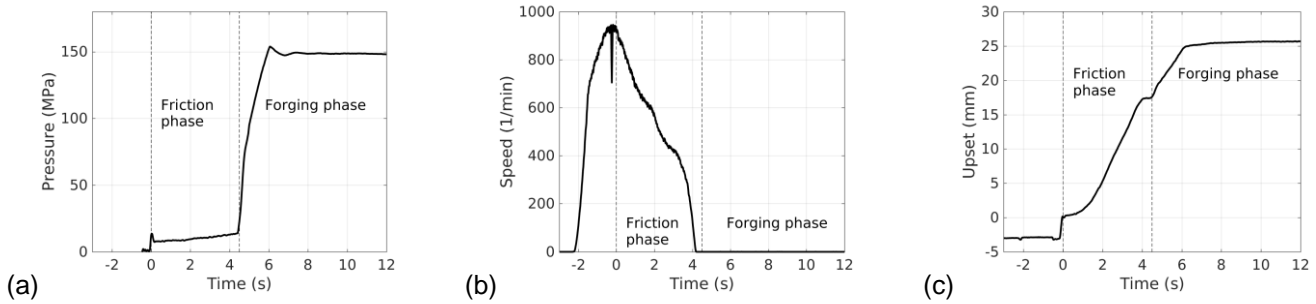
Figure 3:   Welding parameters of Mo welding trial, pre-heated to 400 °C/900 min⁻¹: (a) axial pressure, (b) weld speed, and (c) upset course as response value. A strong upset rate of 7 mm/s during the friction phase is observed.

With the achieved results a detailed analysis of the weld parameter requirements was not possible and therefore the following small-size experiments were performed to:

- Identify reasons for the occurring motor overload and preliminary spindle stall.
- Examine the influence of the material by comparing Mo and TZM.

Molybdenum and TZM small-size formats

The pressure course for the following Mo experiments was kept constant according to Figure 2a, while the friction speed was varied (2,500, 2,600, and 2,750 min⁻¹). The results in Figure 4a show comparable power distributions, however, with different maximum values. That means a higher speed increases the specific weld power and consequently the specific weld energy rises from 55 to 65 and 71 J/mm^2. The measured total upsets increased accordingly from 2.7 to 3.9 and 5.2 mm as shown in Figure 4b. Most of the upset occurred during the forge phase.

The TZM experiments were performed analogously to the Mo experiments, but almost a twice as high level of friction- and forge pressure (Figure 2a) was required for successful welds. The same phenomenon with similar power course that varied in maximum values and hence total weld energy (Figure 5a) was observed. 75, 83, and 89 J/mm^2 resulted in 3.9, 5.4, and 7.0 mm upset (Figure 5b).
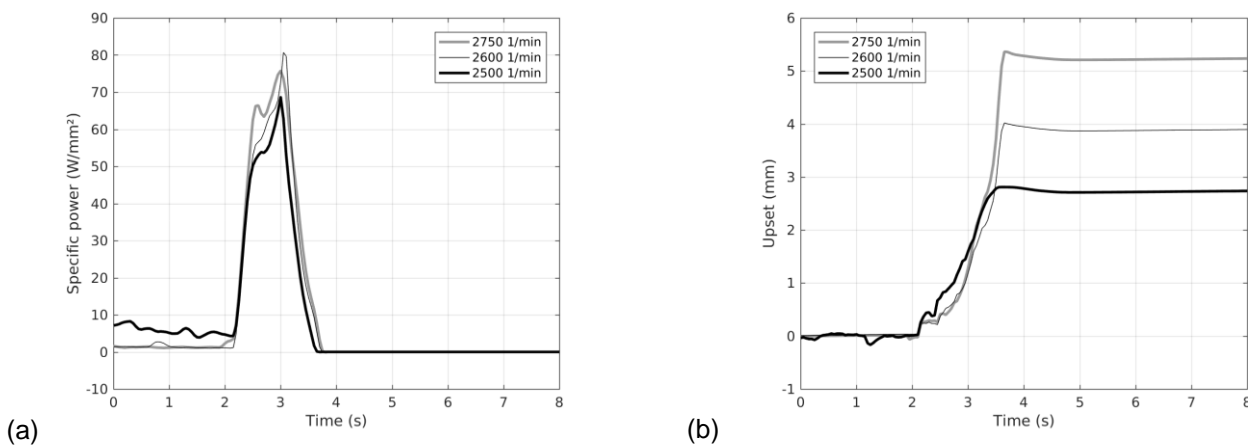

Figure 4:   Influence of the welding speed (2,500, 2,600, 2,750 min⁻¹) of Ø 12 mm Mo samples on the (a) specific weld power and (b) increase in upsets (2.7, 3.9, 5.2 mm).

(a)   (b)
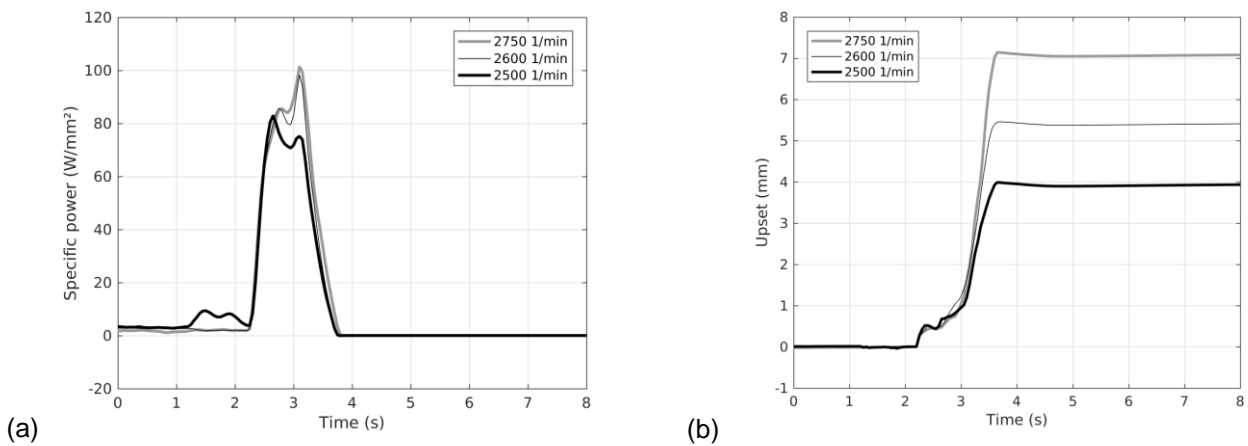
Figure 5:   Influence of the welding speed (2,500, 2,600, 2,750 min⁻¹) of Ø9 mm TZM samples on the (a) specific power, which results in large differences in (b) upsets (3.9, 5.4, 7.0 mm)

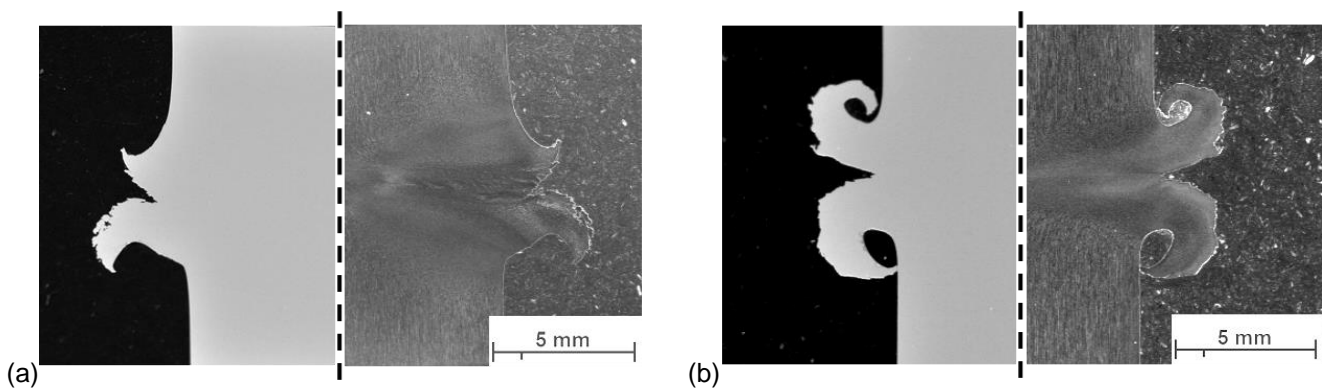(a)   (b)

Figure 6:   Micrographs of friction welded (a) Mo (2,750 min⁻¹) and (b) TZM (2,750 min⁻¹) small-size samples. Both pictures show a polished section on the left, where sound joints without defects are observed. The same area etched on the right shows the plasticized and deformed microstructure.

Figure 6 shows micrographs of representative Mo and TZM welds, both welded at 2,750 min⁻¹. A defect-free joint is observed in the polished sections and the etched sections show a sound weld zone and flash formation.

As observed in the medium-size experiments, a delayed initiation of the forge phase may result in an interruption of the energy input, during which the material cools down and no upsetting occurs. A forging into the turning spindle as employed in the small-size experiments on the other hand, creates a beneficial "energy burst," as observed by the second peak in the power courses of Figure 4a and Figure 5a. To investigate the influence of power progression, the spindle deceleration and the force gradient were varied. Slower spindle deceleration resulted in prolonged welding phases which lead to larger upsets. The in-situ pre-heating phase was excluded for estimating the specific weld energy, since the heat dissipation reached an equilibrium with the inserted power by friction. The calculated values therefore represent the energy input during the friction and forging phase.
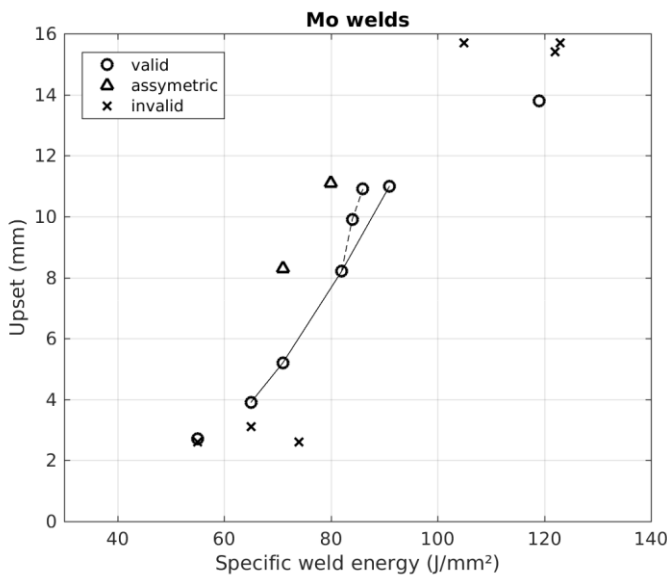
Figure 7:   Display of all Mo trial welds, resulting upset as response to specific weld energy. The best results were achieved with 4,000 min^{-1}s^{-1} deceleration and 7.5 kN/s force gradient, indicated by the solid line. The result of an increased force gradient (7.5, 8, and 8.5 kN/s) is observed by the dashed line. All other points have to be considered invalid due to different reasons.

Figure 7 shows the resulting upset over specific weld energy of all performed Mo welds. In the lower regime insufficient bonding is observed if the upset is lower than 4 mm independent from weld energy. It is assumed that below 4 mm upset the impurities are not completely expelled into the flash and the joint quality is deteriorated. If the welding energy is increased to over 90 J/mm^2, excessive plasticization leads to an instable process with upset rates larger than 20 mm/s and the upset reaches values larger than 12 mm. Between the lower and higher upset threshold, valid welds were produced which are visualized by the solid line (spindle deceleration: 4,000 min^{-1}s^{-1}, forge force gradient: 7.5 kN/s). If the forge force gradient was increased from 7.5 to 8 and 8.5 kN/s (dashed line), upsets increased despite little change in weld energy. The inherent sudden plasticization lead to an asymmetric flash formation in some cases, shown by the triangle marks. Small instabilities during the process caused an angular misalignment of the welding interface and as a consequence these trials shortened more compared to symmetric welds.

These observations show that:

- Mo reacts very sensitively to small changes of the process parameters.
- The specific weld energy may be a parameter for comparison, but only if the forge condition is defined and constant.
- The forge condition with its parameters forge point, spindle deceleration and forge force are equally important for RFW of Mo.

TZM allows larger variations of welding parameters for producing successful welds. It was possible to vary the friction pressure, the force gradient and the spindle deceleration. The TZM results are summarized in Figure 8. Analogously to Mo, a minimum upset of 4 mm was required for sound joining. On the upper scale, the process became instable for upsets exceeding 12 mm. In the center region of the diagram a change in friction pressure from 110 to 125 MPa (downward and upward pointing triangles, respectively) increased the upset values independently from specific weld energy. The same
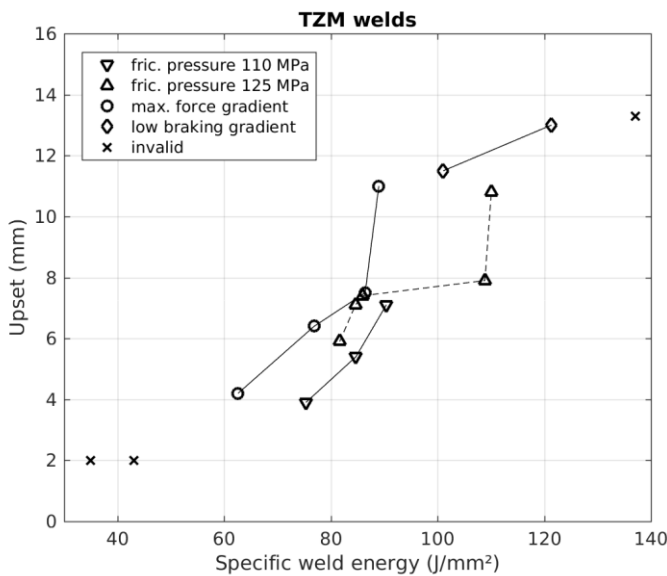
Figure 8:   Display of all TZM trial welds, resulting upset as response to specific weld energy. The main results are observed with 110 MPa friction pressure and 125 MPa. An increased friction pressure lifts the resulting upsets to higher values. Applying the forge force fast (max. gradient of 50 kN/s) also increases the upset in relation to the specific weld energy. A slower braking gradient increases both energy and upset.

effect is observed if the forge force gradient was increased to the machine's maximum capability (resulting in 50 kN/s), as observed by the circle marks. Lowering the spindle deceleration from 4,000 to 3,000 and 2,500 $min^{-1}s^{-1}$ extended the process time, hence the specific energy and resulting upset increased also.

The experiments with TZM show that:

- Higher friction pressures are required compared to Mo.
- Similarly to Mo, the specific weld energy may be suitable to compare welds with identical forge conditions.
- The alteration of force gradient and deceleration influence the resulting upset independently from specific weld energy.

Discussion

Upset behavior

In respect to the results and prior investigations [14], an explanation for the sudden plasticization which causes the observed high upset rates of Mo and TZM is required. Starting from theory, the establishing temperature field in the material due to the generated heat by friction could be a first indicator.

Combining heat capacity c_P, density ρ, and thermal conduction coefficient λ to one coefficient yields the thermal diffusivity $\alpha = \lambda/\rho c_P$. The thermal diffusivity is a measure for the heat transfer rate and, in a sense, it is a measure for thermal inertia. Molybdenum exhibits a low heat capacity but high thermal conductivity and the thermal diffusivity accounts to 53 mm^2/s. To demonstrate the implications of this value, a comparison to low-carbon steel (α = 14 mm^2/s) is drawn: A simple transient heat conduction
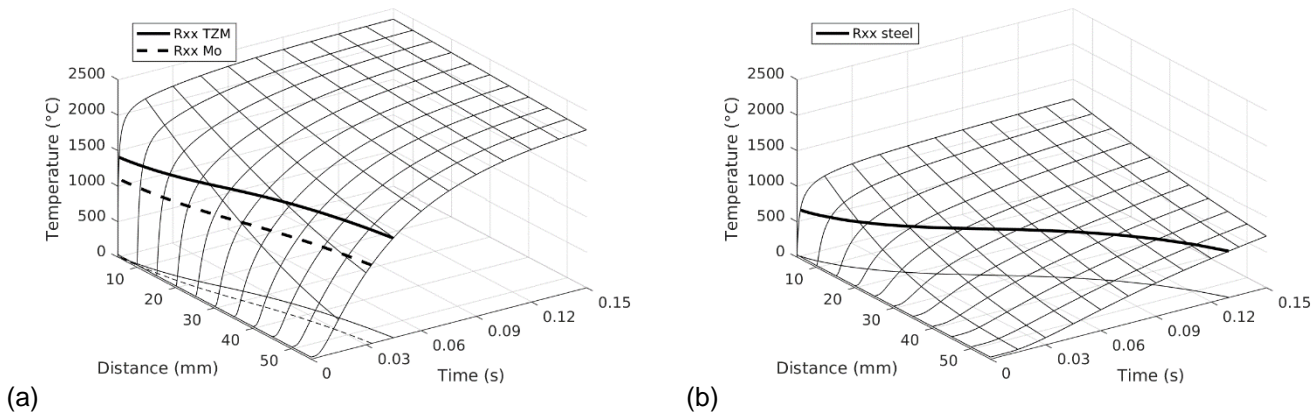
Figure 9:   Schematic comparison of the developing temperature fields between (a) molybdenum and (b) low-carbon steel with boundary conditions T_{max} = 0.9 T_m at position 0 mm. The exceedance points of the recrystallization temperatures (TZM: 1,400 °C, Mo: 1,100 °C, steel: 650 °C) are indicated by the solid and dashed lines, respectively.

calculation [16] visualizes the evolution of the temperature field in time and distance from a heat source, as displayed in Figure 9. The exceedance of a certain temperature, exemplarily the recrystallization condition, T_{Rxx} is reached much faster and in a wider range in Mo than in steel. As a consequence for friction welding, with rising thermal diffusivity a larger volume is heated in shorter time, exceeds the shear strength, and starts to plasticize.

With the present observations of the trial welds and the discussed influence of the transient heat dissipation, a premise may be formulated: The thermal diffusivity determines the manifesting temperature field. The temperature field governs plasticization, which starts when a certain temperature is exceeded. That means for Mo and TZM with their high thermal diffusivities, a large volume starts to plasticize suddenly, which may cause instable process conditions. As a consequence, friction welding of Mo and TZM requires the energy input to be rapid and thus the process time to be short to produce a high spatial temperature gradient in the weld specimen.

Scalability of parameters

As discussed previously, the progression of welding power is of crucial importance. To scale the process to a larger geometry, the following characteristics have to be considered:

1. The specific welding energy (J/mm²) during the welding phase.
2. The forge condition.
3. A short welding time to minimize the heat dissipation.
4. Different thermal boundary conditions due to a different geometry and different clamping conditions will influence the heat dissipation, but are difficult to estimate.

Figure 10 displays the 1.5 s welding phase of the small-size Mo trial with 2,750 min⁻¹ spindle speed which resulted in a sound joint (see Fig. 6a). Up-scaling from 113 mm² to 4,400 mm² (secondary y-axis) increases the required total weld energy from 8.35 to 325 kJ. Further, the curve peaks at 333 kW drive power for the large cross section. Leading this assumption demonstrates that the used 150 kW RFW machine did not provide the required power for a pure direct drive of the medium-size samples which easily explains the stall during welding.
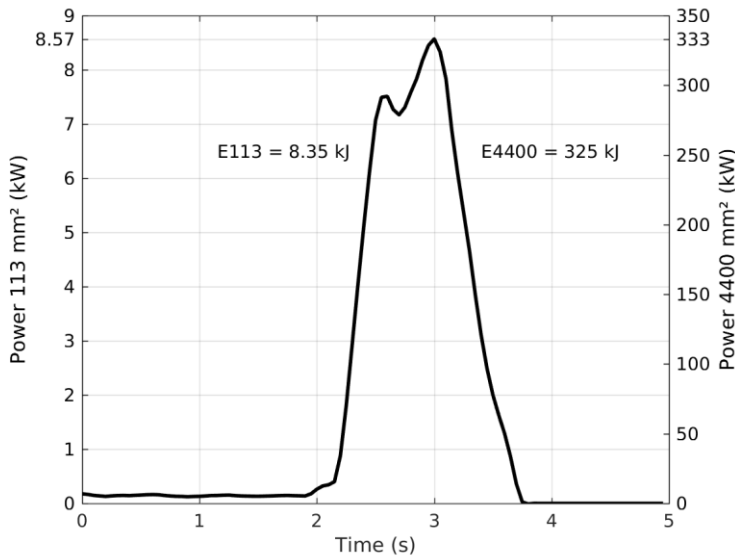
Figure 10: Scaling the small-size process from 113 mm² to 4,400 mm² results in 325 kJ total weld energy and reveals a peak power of 333 kW.

Summary and conclusion

The process of friction welding is very stable and established for a large range of materials like steels, or titanium alloys, among others. Compared to these materials, Mo and TZM proved to be more challenging to establish a friction welding process due to their largely different thermo-physical and -mechanical properties, most of all their high thermal diffusivity. This work presents experiments of medium-size tubes on an industrial DDFW machine and small-size samples on an adapted laboratory machine to investigate the weldability of Mo and TZM. Successful welds as part of the investigation are shown in Figure 11. Concerning the material behavior, the following is summarized:

1. Mo and TZM plasticize extensively during the DDFW processes, which is mostly due to the high thermal diffusivity of Mo. This causes a large volume to exceed the shear strength and reduces the parameter windows for a successful process.
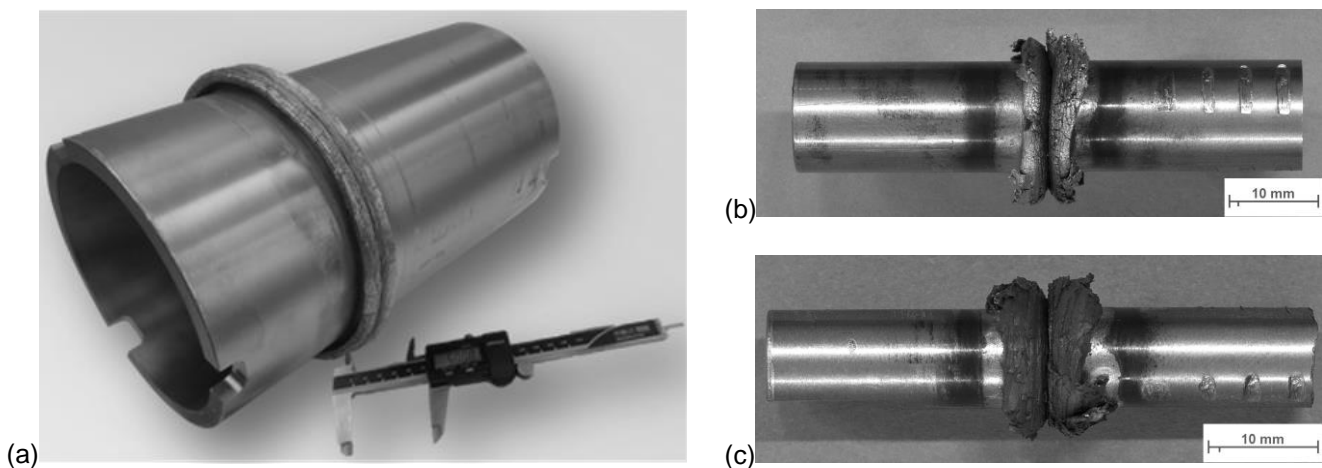

Figure 11: Macro pictures of successful welds: (a) medium-size Mo tubes, (b) small-size Mo rod, and (c) small-size TZM rod

2. Concerning the welding process, the plasticized volume is to be kept to a minimum to ensure a stable flash formation [17]. Hence, a short process time is sought to establish a sufficient spatial temperature gradient.
3. The process time relates directly to the required drive power; a shorter process time will result in a higher drive power peak to balance the energy input.

Through the more versatile process conditions in small-size, insights into process parameters and their influence on the weld were gained and the following was concluded:

1. If the pre-heating phase is taken into account of calculating the specific weld energy, the values are not comparable. Therefore, the important part in direct drive processes is the later friction and deceleration period, which were considered for assessing the friction welding processes.
2. Upset thresholds were determined between 4 and 12 mm for small-size specimens of Mo and TZM. Below 4 mm insufficient bonding was observed, above 12 mm the weld process became unstable.
3. Specific weld energy can be a starting point value for the comparison of IFW and DDFW, but specific weld energy alone was insufficient to fully describe the DDFW process. If the forge condition (forge force gradient and spindle deceleration) was altered, the resulting upset changed despite similar specific weld energies. These deviations demonstrate that the manner of energy input—thus the forge condition—is important for describing the weld process.
4. The point of forge force initiation needs to be upon deceleration start (forging into the turning spindle) to create an energy burst for effective welding. If the forge force was applied after the spindle stop, the plasticization interrupted and the joint formed incompletely.
5. A decrease of the spindle deceleration from 4,000 to 3,000 $min^{-1}s^{-1}$ resulted in a 0.25 s longer process time and doubled the resulting upset. Therefore, a fast spindle deceleration is preferable as the excessive time during braking increases the plastically deformed volume around the bonding plane.
6. The maximum force gradient of 50 kN/s was applicable to TZM but not to Mo. In that case the plasticization of the latter became unstable. With a controlled force gradient between 6 and 7.5 kN/s successful welds were achieved, while the steeper force gradient produced better results.

Outlook

The predicted power course for medium-size samples should be put into experiment to confirm the conclusions of this work. The comparison of specific welding energies of different metals during RFW and their resulting upsets could further be used to enhance the presented theory about the influence of thermal diffusivity.

For deeper understanding of the plasticization behavior of Mo and TZM, numerical simulation will be an important asset. Therefore, temperature dependent thermo-mechanical properties up to the melting point are required.

Acknowledgment

References

1. E. M. Savitskii and G. S. Burkhanov, *Physical Metallurgy of Refractory Metals and Alloys.* Boston,
    MA: Springer US, 1970

2. M. Nagae, T. Yoshio, J. Takada, and Y. Hiraoka, "Improvement in Recrystallization Temperature and
    Mechanical Properties of a Commercial TZM Alloy through Microstructure Control by Multi-Step
    Internal Nitriding," *Mater. Trans.*, vol. 46, no. 10, pp. 2129–2134, 2005

3. "Molybdän Werkstoffeigenschaften und Anwendungen," 2013

4. A. J. Bryhan, "Joining of Mo Base Metal and Factors Which Influence Ductility." Exxon Production
    Research Co., Houston, TX, 1986

5. S. Primig, H. Leitner, H. Clemens, a. Lorich, W. Knabl, and R. Stickler, "On the Recrystallization
    Behavior of Technically Pure Molybdenum," *Int. J. Refract. Met. Hard Mater.*, vol. 1, pp. 1–9, 2009

6. A. Ambroziak, "Friction welding of molybdenum to molybdenum and to other metals," *Int. J. Refract.
    Met. Hard Mater.*, vol. 29, no. 4, pp. 462–469, Jul. 2011

7. B. Tabernig and N. Reheis, "Joining of molybdenum and its application," *Int. J. Refract. Met. Hard
    Mater.*, vol. 28, no. 6, pp. 728–733, Nov. 2010

8. M. M. Schwartz, "Friction Welding," in *Metals Joining Manual*, McGraw-Hill Book Company, 1979, p.
    6.1-6.51

9. M. Maalekian, "Friction welding – critical assessment of literature," *Sci. Technol. Weld. Join.*, vol. 12,
    no. 8, pp. 738–759, Nov. 2007

10. A. Ambroziak, "Temperature distribution in friction welded joints of dissimilar refractory metals," *Adv.
    Manuf. Sci. Technol.*, vol. 26, no. 3, pp. 39–54, 2002

11. Manufacturing Technology Inc., "Friction welding," 1999

12. V. R. Dave, M. J. Cola, and G. N. Hussen, "Heat generation in the inertia welding of dissimilar tubes,"
    Weld. J., vol. 80, no. 10, p. 246s–252s, 2001

13. F. Pixner, M. Stütz, J. Wagner, N. Reheis, and N. Enzinger, "Comparing Molybdenum and Steel in
    Rotary Friction Welding using an FSW Machine," in *22. Erfahrungsaustausch Reibschweissen*, 2017

14. M. Stuetz, N. Enzinger, J. Wagner, N. Reheis, H. Kestler, and E. Raiser, "Rotary Friction Welding of
    Large Molybdenum Tubes," *Proc. 10th Int. Conf. Trends Weld. Res.*, pp. 153–156, 2016

15. L. Wenya and W. Feifan, "Modeling of continuous drive friction welding of mild steel," *Mater. Sci.
    Eng. A*, vol. 528, no. 18, pp. 5921–5926, 2011

16. C. Xie, "Interactive Heat Transfer Simulation for Everyone," *Phys. Teach.*, vol. 50, no. 4, pp. 237–
    240, 2012

17. K. Mucic, F. Fuchs, and N. Enzinger, "Process optimization for linear friction welding of high strength chain," in *EUROJOIN Conference*, 2012, pp. 157–166